



# Mechanical and ballistic characterization of high-density polyethylene composites reinforced with alumina and silicon carbide particles

Bruno Figueira de Abreu Ferreira CARDOSO<sup>1</sup>, Flávio James Humberto Tommasini Vieira RAMOS<sup>2</sup>, Pedro Henrique Poubel Mendonça da SILVEIRA<sup>1</sup>, Anthony Garotinho Barros Assed Matheus de OLIVEIRA<sup>1</sup>, André Ben-Hur da Silva FIGUEIREDO<sup>1</sup>, Alaelson Vieira GOMES<sup>1,\*</sup>, and Valdir Florêncio da VEIGA-JUNIOR<sup>1</sup>

<sup>1</sup> Military Institute of Engineering - IME, Praça General Tibúrcio, 80, Praia Vermelha, Urca, 22290-270, Rio de Janeiro, RJ, Brazil

<sup>2</sup> Instituto de Macromoléculas Professora Eloisa Mano, Universidade Federal do Rio de Janeiro, Avenida Horácio Macedo, 2030 – Centro de Tecnologia, Bloco J, Ilha do Fundão, 21941-598, Rio de Janeiro, RJ, Brazil

\*Corresponding author e-mail: [alaelson@ime.eb.br](mailto:alaelson@ime.eb.br)

**Received date:**  
24 March 2022  
**Revised date**  
17 May 2022  
**Accepted date:**  
24 May 2022

**Keywords:**  
Ballistic resistance;  
Mechanical properties;  
DOP;  
HDPE;  
Alumina

## Abstract

This article explores the ballistic and mechanical performance of HDPE matrix composites reinforced with alumina and silicon carbide particles, to be used as lightweight body armor. The composites were processed by hot pressing, with the addition of ceramic fillers in fractions of 0, 40, 50, 60, 70, and 80 wt%, forming the sample groups A00, A40, A50, A60, A70, and A80. After processing, the composites were evaluated by tensile tests, Izod impact, and Shore D hardness. In addition, depth of penetration (DOP) and energy absorption tests were performed with chronograph simulating .22 ammunition in the ballistic test. Samples A80 and A70 had the lowest DOP result (15.98 mm and 17.98 mm respectively) indicating that these samples had the best ballistic performance. Mechanical tests performed on samples A00, A40, A50, and A60 showed that the deformation and tensile strength were reduced with the addition of ceramic reinforcement. Impact resistance also decreased. Shore D hardness showed a considerable increase in hardness of A40, A50, and A60 compared to A00.

## 1. Introduction

Firearm injuries have been a universal problem from a human, medical and economic point of view [1,2]. Its incidence is different between countries and its characteristics vary in several aspects [3], being often lethal when affecting victims [4]. Brazil has one of the highest homicide rates in the world. According to data from the Ministry of Health of Brazil, 58,138 people died from homicide in Brazil in 2015 (28.4 per 100,000 population), in which about three quarters were killed by firearms [5].

One of the biggest challenges in the military sector is to obtain efficiency in the weight versus ballistic efficiency ratio of bulletproof vests. To achieve this feat, a multilayer reinforcement system (MAS) is normally used, in which this model has a front layer made of advanced ceramic. This material has high hardness and can resist the initial impact of the projectile and damage it [6]. Modern ballistic vests are made from advanced ceramics, where the most common are alumina ( $Al_2O_3$ ), silicon carbide (SiC), and boron carbide ( $B_4C$ ) [7,8], in addition to being reinforced with fabric fibers and/or natural fibers [9-12]. Three factors make ballistic armor efficient: mobility, penetration resistance, and high impact absorption. One of the biggest challenges in making these shields is to improve these factors so as not to harm other properties. Thus, the development of new composites can help provide lighter and more efficient equipment compared to conventional protections of monolithic plates [13-17].

The low porosity of advanced ceramics provides superior mechanical properties such as high dynamic compressive strength, high hardness, and low density. Alumina is one of the most used ceramics due to its easy processing, low cost, and diversity of application sectors, however, it has low toughness and fracture energy. Its low fracture toughness can become a limiting factor for its application [18]. The addition of silicon carbide (SiC) to alumina showed better results compared to research with the addition of zirconia to alumina. Silicon carbide (SiC) increased the modulus of elasticity of the material, exhibiting low density, greater flexural strength, greater hardness, and fracture toughness [19-22]. The use of a thermoplastic polymer with alumina, forming a composite, can be an alternative to the problem of low fracture toughness of ceramic [23]. It is important to develop alternatives to improve the strength of a multi-layer ballistic protection system. The low toughness and brittleness of ceramics result in less resistance to subsequent ballistic impacts, especially at points close to the previous impact. High-density polyethylene (HDPE) has several advantages over other polymers, such as low production cost, excellent chemical, physical, mechanical, and thermal properties, good flexibility, and considerable hardness at low temperatures. Research has shown that the addition of alumina as a reinforcing filler in the HDPE matrix promotes changes in the thermal, physical and mechanical properties of the composite, as well as changes in the crystallinity of the polymer. The effects presented by the authors showed an increase in the modulus of elasticity of up to 501% compared to the pure matrix [24-26].

This paper presents a study of HDPE matrix composite reinforced with alumina (Al<sub>2</sub>O<sub>3</sub>) particles and silicon carbide (SiC) particles and evaluates the mechanical and ballistic behavior of this composite, to be used as lightweight body armor. The brittle behavior of ceramic materials motivated the use of HDPE matrix composites capable of mitigating problems such as toughness and ballistic strength [27-29].

## 2. Experimental

### 2.1 Sample preparation

The materials used to make the composites were alumina Alundum RR (A620), 60 mesh, hardness 9.25 (Fisher Scientific, USA), HDPE IE59U3 powder (Braskem, Brazil) and silicon carbide (SiC) powders SIKA SINTEX 13C (Fiven, Norway) with 100 μm average diameter.

Alumina, silicon carbide and HDPE were mixed by mechanical stirring for 10 min in a vertical milling machine. Homogenization took place during along with bonding of the HDPE with the ceramic particles by friction stir weld. Percentages of alumina between 39 wt% and 79 wt% plus 1 wt% of silicon carbide were used, and the samples were identified according to Table 1. A sample with 100% HDPE was added for control. Table 1 also presents the alumina volume fractions for each composite.

The alumina, silicon carbide, and HDPE mixtures were hot-pressed, at 200°C, in a SOLAB SL-11 press with the aid of a mold (51 mm in diameter and 5 mm in thickness). Figure 1 shows the loads and times used in this process. Before unloading the samples, another stage of compression at room temperature (25°C) was performed, using a load of 30 kN for 10 min.

### 2.2 Ballistic tests

The depth of penetration test (DOP) was used in this study to evaluate the ballistic performance of composites. The depth of penetration value is determined by the depth of the impact cavity created by the material positioned behind the target [30,31]. The samples used in the ballistic tests were produced with the dimensions as presented earlier in section 2.1 (51 mm in diameter and 5 mm thickness). Ballistic tests were carried out with compressed air rifle model SSS and Gunpower (Figure 2(a)) with two communicating cylinders (0.5 L and 6 L) and an estimated pressure of 28 MPa. Lead projectiles 0.22 LR caliber (Figure 2(b)), with a mass of 3.3 g, were used. The velocity on each shot was measured using a Chrony Model MK3 Ballistic Air Chronograph (Figure 2(c)) device with an accuracy of 0.15 m·s<sup>-1</sup>. The distance between the air rifle and the composite was 5 m. The samples were fixed on a wooden board, as shown in Figure 3. The wooden board has the function of housing the projectile, in case the projectile passes through the sample, allowing the quantification of the penetration depth (DOP). Images of the samples after penetration were recorded with a digital camera. The energy absorbed by the target is calculated using Equation (1):

$$E_{\text{abs}} = \frac{m_p(v_i^2 - v_r^2)}{2} \quad (1)$$

Where  $E_{\text{abs}}$  is the absorbed energy by the composite (J),  $m_p$  is the projectile mass (g),  $v_i$  is the impact speed and  $v_r$  is the residual speed (m·s<sup>-1</sup>). A second ballistic shot was performed to measure the depth of penetration (DOP) in each disc. After the bullet hits the samples, it lodges inside the wood plate. Measuring bullet penetration in the wood plate is important to understand how much the composite was able to withstand the ballistic impact [32]. To perform the ballistic tests, 7 samples were used for each group.

Table 1. Samples identification.

Identification	Composition
A00	100% HDPE
A40	HDPE + 39 wt% Al <sub>2</sub> O <sub>3</sub> + 1 wt% SiC
A50	HDPE + 49 wt% Al <sub>2</sub> O <sub>3</sub> + 1 wt% SiC
A60	HDPE + 59 wt% Al <sub>2</sub> O <sub>3</sub> + 1 wt% SiC
A70	HDPE + 69 wt% Al <sub>2</sub> O <sub>3</sub> + 1 wt% SiC
A80	HDPE + 79 wt% Al <sub>2</sub> O <sub>3</sub> + 1 wt% SiC

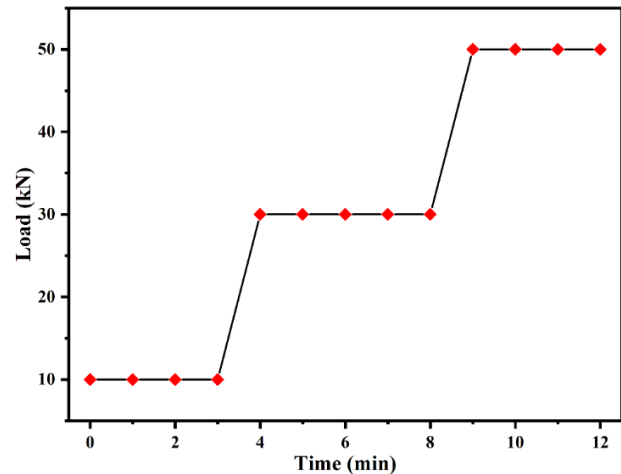
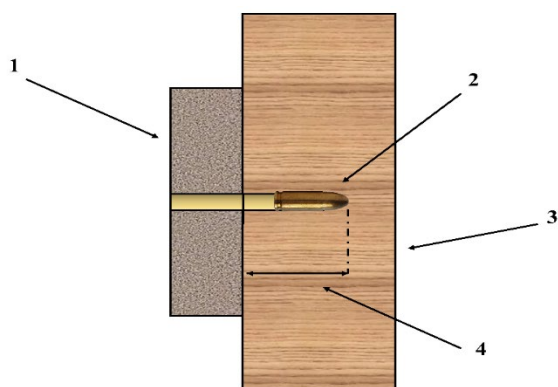


Figure 1. Relation of loading time versus sample compression load.



Figure 2. (a) Chrony Model MK3 Ballistic Air Chronograph, (b) Lead projectiles 0.22 LR caliber, and (c) Compressed air rifle model SSS.



**Figure 3.** Positioning scheme for ballistic testing (1) composite, (2) projectile, (3) wood plate, and (4) depth of penetration (DOP).

## 2.3 Mechanics tests

### 2.3.1 Tensile tests

All the tensile tests were performed following standard methods. The tensile tests were carried out at  $5 \text{ mm}\cdot\text{min}^{-1}$  in a Universal Testing Machine (Instron, Brazil), according to ASTM D 638-14 standard [33], using type IV samples, with dimensions of  $36 \text{ mm} \times 6 \text{ mm} \times 4 \text{ mm}$ . To perform the tensile tests, 7 samples were used for each group.

### 2.3.2 Izod impact test

For Izod impact tests, 7 specimens with dimensions of  $63.5 \text{ mm} \times 12.7 \text{ mm} \times 6 \text{ mm}$  and a  $45^\circ$  notch were produced for each group. The test was performed in accord with ASTM D 256-10 standard [34] (Resil Impact, Korea) using a 5.5 J hammer, and a steel mill was used to print the dimension of 2.54 mm deep in a  $45^\circ$  angulation [35,36].

### 2.3.3 Shore D Hardness test

The hardness test was carried out using a Shore-D hardness tester according to ASTM D 2240-15 standard [37], the diameter of the steel indenter was 1.4 mm,  $30^\circ$  conical pointed tip with a radius of 0.1 mm. The penetrated depth of the indenter mark was used to characterize the hardness value. The test was performed at room temperature, considering the maximum hardness value [28]. Five indentations were performed in different regions of the sample, for the average calculation of hardness.

### 2.3.4 Scanning Electron Microscopy (SEM)

After the ballistic test, the fracture surfaces of the samples were analyzed by scanning electron microscopy. The samples were cut in specific regions preserving the fracture surface after firing. A Quanta FEG 250 microscope (Termo Fisher Scientific, USA) was used, equipped with a field emission electron gun, operating at 5 kV in low vacuum mode (at 80 Pa pressure). The purpose of the analysis was to identify the types of fractures present in these composites

after ballistic impact. The samples were coated with a thin gold layer using a cathodic sputter model ACE 600 (Leica, Germany) for 30 min.

## 3. Results and discussion

### 3.1 Ballistic performance

All the shots went through the samples. For each composition, seven samples were used. Figure 4 shows the energy absorption during the ballistic impact, followed by Table 2, showing the values of disk mass ( $m_c$ ), projectile mass ( $m_p$ ), initial speed ( $V_i$ ), residual speed ( $V_r$ ), and absorbed energy ( $E_{abs}$ ) for each composition.

The composites had low energy absorption in general, however, the A80 sample had the highest energy absorption value during ballistic impact. Samples A00, A60, and A70 presented values in the same energy absorption range. As the concentration of  $\text{Al}_2\text{O}_3$  is increased, the energy absorption in penetration is also high, except for A40 which showed a reduction in energy and an increase in penetration depth. This low concentration of alumina in the matrix and consequent reduction in energy absorption is due to the introduction of defects in the matrix, without a significant contribution to the increase in strength [24,25]. Only in the composition of the A80 group that there was a significant increase in energy absorption.

The A80 samples showed the best ballistic performance, due to the lower penetration of the projectile, followed by A70 and A60. The A40 had the worst performance among all groups, being worse than the A00. According to Lins *et al* [38] the addition of  $\text{Al}_2\text{O}_3$  to HDPE causes an increase in the elastic modulus of the composite, improving mechanical properties, but high levels of  $\text{Al}_2\text{O}_3$  in the HDPE matrix cause agglomerates to spread throughout the composite, impairing the mechanical performance of the material.

Corroborating the results obtained for the samples with high reinforcement loading, Figueiredo *et al* [23] point out that low concentrations of alumina do not contribute significantly to the increase in penetration resistance. Additions above 60 wt% of  $\text{Al}_2\text{O}_3$  contribute to the crystallization of the regions around the particles, increasing hardness and improving ballistic performance.

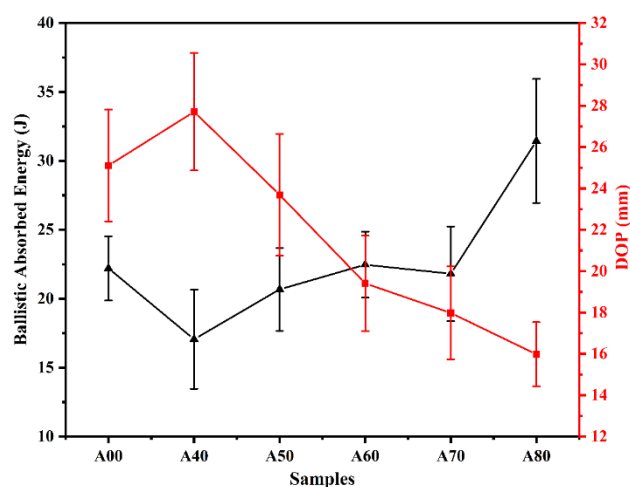


**Figure 4.** Ballistic absorbed energy and DOP values for composites.

**Table 2.** Results of ballistic impact measuring the  $E_{abs}$ .

SAMPLE	$M_c$ (g)	$m_p$ (g)	$V_i$ ( $m \cdot s^{-1}$ )	$V_r$ ( $m \cdot s^{-1}$ )	$E_{abs}$ (J)	DOP (mm)
A00	$7.92 \pm 0.20$	$3.36 \pm 0.06$	$253.90 \pm 13.89$	$225.00 \pm 17.27$	$23.25 \pm 2.33$	$25.11 \pm 2.70$
A40	$12.29 \pm 1.76$	$3.36 \pm 0.06$	$256.40 \pm 4.55$	$234.77 \pm 4.33$	$17.85 \pm 3.60$	$27.11 \pm 2.84$
A50	$13.31 \pm 1.11$	$3.36 \pm 0.06$	$253.98 \pm 2.38$	$227.32 \pm 4.39$	$21.56 \pm 3.01$	$23.69 \pm 2.94$
A60	$14.81 \pm 1.74$	$3.36 \pm 0.06$	$257.26 \pm 3.95$	$228.48 \pm 3.19$	$23.48 \pm 2.40$	$19.41 \pm 2.30$
A70	$15.75 \pm 3.12$	$3.36 \pm 0.06$	$257.98 \pm 2.30$	$230.79 \pm 2.58$	$22.32 \pm 3.43$	$17.98 \pm 2.25$
A80	$21.78 \pm 1.22$	$3.36 \pm 0.06$	$257.86 \pm 3.39$	$219.15 \pm 6.18$	$32.49 \pm 4.50$	$15.98 \pm 1.55$

Figure 5 shows the samples after the ballistic test impact. Samples A00, A40, A50, A60 and A80 did not show long-range cracks and fractures due to impact. Sample A70 had a crack that starts in the impact region and extends to the edge of the sample.

The ballistic performance of lightweight armors produced with thermoplastic polymers and ceramic reinforcements has been studied by several researchers in recent years. Chagas *et al* [57] investigated the ballistic performance of lightweight armors made of ultra-high molecular weight polyethylene (UHMWPE) reinforced with boron carbide ( $B_4C$ ) nanoparticles in small fractions (0, 0.01, 0.05, and 0.1 wt%). The authors reported that the addition of 0.05 wt% of  $B_4C$  promoted an improvement in ballistic performance, in which a depth of penetration (DOP) value of approximately 14 mm was presented against .22 LR ammunition, a value slightly higher than that found in the present work for the A80 group. Fejdyś *et al* [58] investigated the ballistic performance of UHMWPE matrix composites reinforced with alumina and silicon carbide particles, in which the composites

underwent an accelerated aging process. After accelerated aging considering a condition of 6 years of use, the composites showed a reduction in ballistic performance. Thus, the authors related the time of use of the lightweight armor with its durability. Oliveira *et al* [32] investigated the ballistic properties of low-density polyethylene composites (LDPE) reinforced with alumina particles in a concentration ranging from 0 wt% to 100 wt%. The authors observed that fractions of 80 wt% and 85 wt% resulted in the best results of ballistic resistance, in which the penetration of an ammunition caliber .22 LR, was almost null. Figueiredo *et al* [55] performed ballistic tests with .22 LR ammunition in UHMWPE/ $Al_2O_3$  composites subjected to gamma radiation at different ratios (0, 25, 50, and 75 kGy). The composites in general showed absorption of ballistic energy around 20% to 30%, results compatible with the present study, however, the addition of 80 wt%  $Al_2O_3$  and 50 kGy of gamma radiation resulted in the absorption of approximately 65%, resulting in improved ballistic performance.

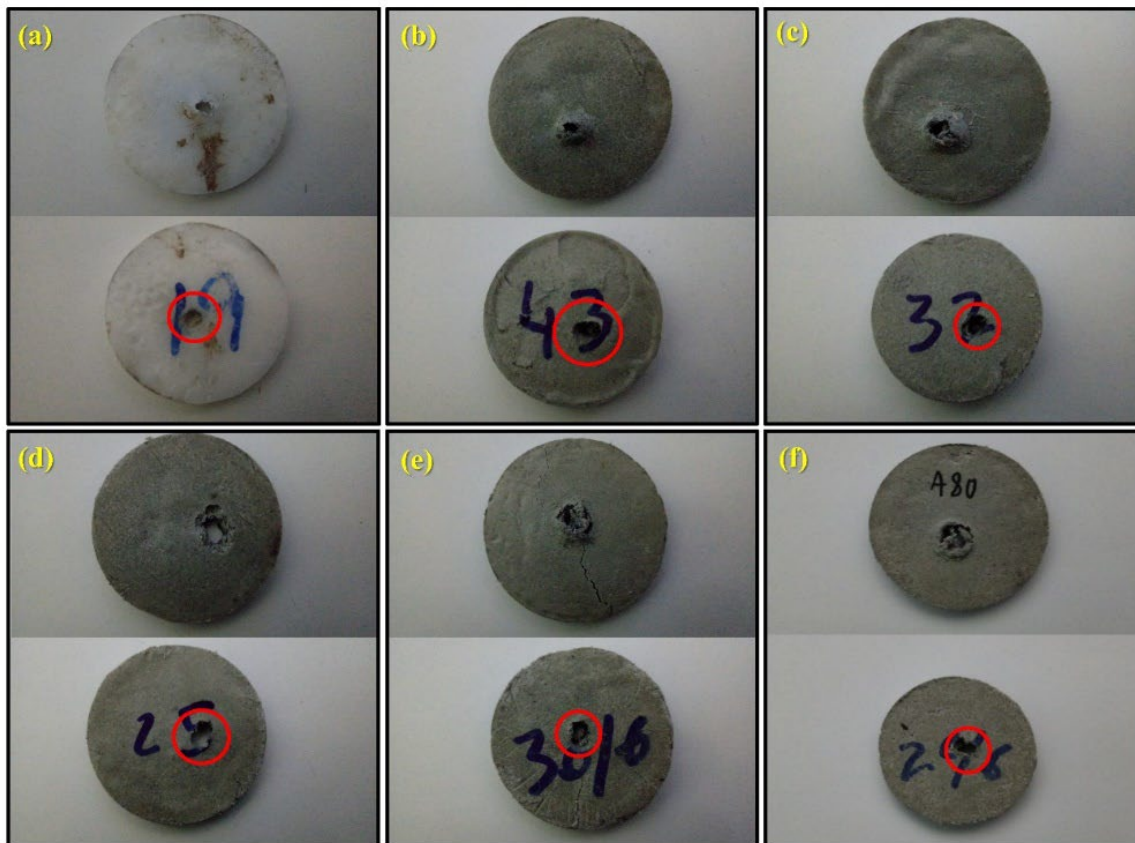


**Figure 5.** Photograph of samples after ballistic test: (a) A00, (b) A40, (c) A50, (d) A60, (e) A70, and (f) A80. Red circles indicate the penetration location. The front view of the sample is indicated by the numbers written on the samples.



### 3.2 Microstructural analysis

Figure 6 shows the fracture surfaces analyzed by SEM. After ballistic testing, the fracture regions were separated for viewing under the microscope. Sample A00 (Figure 6(a)) presents ductile fracture due to the absence of ceramic reinforcements and severe plastic deformation present in the specimen. Sample A40 (Figure 6(b)) shows a debonding of the matrix/particle interface, and also shows cracks in the  $Al_2O_3$  particles, dispersed from the HDPE matrix. Samples A50 and A60 (Figures 6(c) and 6(d)) showed ductile mechanisms related to the propagation of shock wave in the material, in addition to fragile fracture in regions with ceramic reinforcement. Sample A70 showed ductile fracture in the HDPE matrix, and also resulting from the debonding of the ceramic, which can be seen in Figure 6(e). Sample A80 (Figure 6(f)) also had a predominantly fragile fracture, with some small stretches showing ductile fracture.

The interfacial adhesion of the polymeric matrix with the ceramic reinforcements did not occur optimally, as can be seen in Figure 6(b), for example, where there is the presence of ceramic particles detached from the matrix after the ballistic test. A composite with good interfacial adhesion would absorb a greater amount of energy during the ballistic event, besides the composite being able to keep the ceramic particles encapsulated inside the matrix. As an alternative to promote better interfacial adhesion in composites reinforced with ceramic particles, techniques such as extrusion [39] and direct ink writing (DIW) [40] have emerged as potential processing techniques for the production of thermoplastic composites.

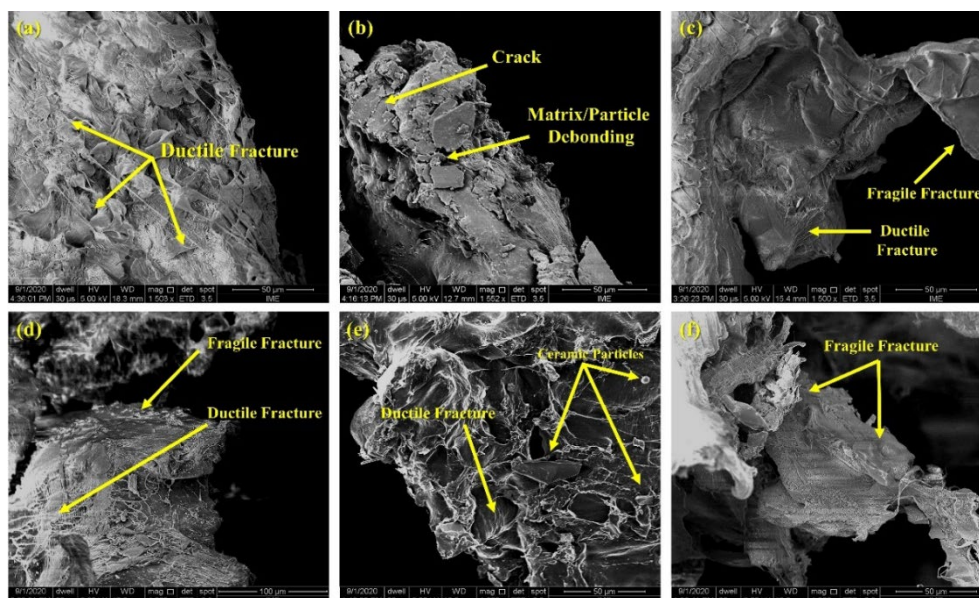
### 3.3 Mechanical characterization of A00, A40, A50, and A60 composites

Mechanical tests could not be performed on samples A70 and A80. The high addition of ceramic reinforcement did not allow the composites to be processed satisfactorily. The A00 samples had a maximum tensile strength of 26.65 MPa, close to that provided by

the manufacturer (27 MPa). Vijay *et al* [41] obtained results of 27 MPa indicating the mechanical stability of pure HDPE. The graph in Figure 7 and the results of Table 3 show the tensile values for the A00, A40, A50, and A60 samples. The deformation of A00 was 1026%, higher than that found by Coutinho *et al* [29] who obtained 800% for HDPE samples processed under the same condition. According to Kaya *et al* [42] a problem related to the plastic deformation tensile test of semi-crystalline polymeric materials, as the deformation mechanism is complex, because the material has crystalline regions randomly arranged between amorphous regions. During the deformation process, the polymer chains stretch until the chains split, resulting in material rupture. This makes thermoplastic polymers reach high strains.

The addition of  $Al_2O_3$  and SiC in HDPE reduced the maximum stress and strain of the composites, as the ceramic reinforcement played a barrier role, preventing the chains from stretching, resulting in a brittle fracture. However, the addition of ceramic reinforcement resulted in greater stability for the composites. One factor that resulted in poor performance in the tensile test was the weak affinity of polymer chains with ceramic particles [43]. The loss of ductility of a composite is a result of the fragility of ceramic materials [32,44,45]. According to Chee *et al* [36] plastic deformation in the polymer matrix is a predominant mechanism in energy absorption, being reduced with the addition of reinforcement. In the case of composites reinforced by ceramic particles, the main deformation process is the displacement between the matrix/reinforcement interface, which provides an increase in the volume of material in the deformation, displacing the particles and generating voids in the matrix [46].

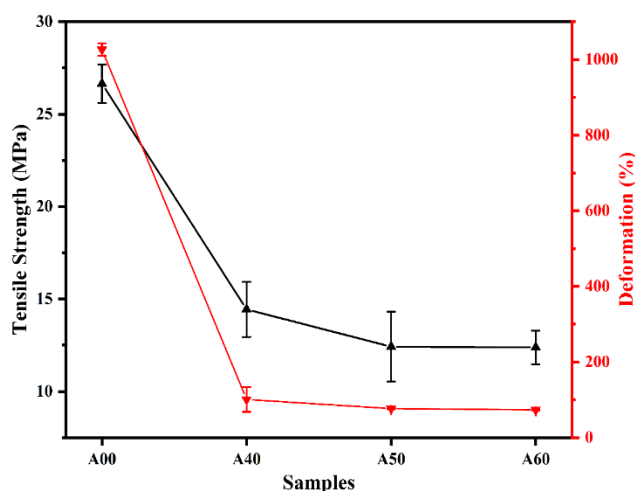
An alternative for greater adhesion of the matrix/reinforcement interface would be the use of compatibilizers. Grison *et al* [47] report that the addition of 2% maleic anhydride (PP-g-MA) in HDPE composites with additions of 9% to 33% of  $Al_2O_3$ , resulted in significant improvements in the mechanical properties of the composites, obtaining resistance values to a tensile strength of 23.24 MPa and 22.20 MPa respectively, results close to those obtained for A00, demonstrating that the use of compatibilizer improves the mechanical properties of HDPE matrix composites [48,49].



**Figure 6.** SEM micrographs of the fracture regions of the shot samples: (a) A00, (b) A40, (c) A50, (d) A60, (e) A70, and (f) A80.

**Table 3.** Mechanical Characterization for the HDPE composites.

Sample	Tensile strength (MPa)	Deformation (%)	Izod energy absorbed ( $\text{J}\cdot\text{m}^{-1}$ )	Shore D Hardness
A00	$26.65 \pm 1.04$	$1026.43 \pm 16.69$	$24.13 \pm 4.20$	$46 \pm 2.50$
A40	$14.44 \pm 1.49$	$100.84 \pm 32.64$	$14.85 \pm 3.08$	$69 \pm 1.30$
A50	$12.42 \pm 1.89$	$76.75 \pm 1.71$	$13.99 \pm 2.81$	$70.80 \pm 1.60$
A60	$12.38 \pm 0.91$	$73.53 \pm 1.63$	$18.31 \pm 3.61$	$72 \pm 1.40$

**Figure 7.** Tensile Strength of A00, A40, A50, and A60 composites.

Regarding the Izod impact test presented in Table 3, the results obtained for the A00 were similar to those of Deepak *et al* [26], for the same test conditions. Semi-crystalline polymers such as HDPE have high tenacity under common conditions of use. However, they are sensitive to the notch made in the specimen, causing the material to harden [50,51].

The standard deviation of the samples was high, demonstrating that there was not good adhesion of the ceramic reinforcement to the polymer matrix. Another factor related to the results of lower impact resistance is the processing of composites. Hot pressing can create internal voids during processing, where even with the elimination of waste gases, it is not always possible to eliminate them completely. During the impact test, the presence of a notch or other stress concentrator can change the stress state of the material, making plastic deformation difficult and reducing the tenacity of the specimen [52]. The reduction in impact energy with increasing ceramic load occurs because plastic deformation decreases with the addition of ceramic load [27].

Shore D hardness results was shown in Table 3. The values obtained for A00 were lower than those established by the manufacturer, where 61 Shore D is established, and in this work 46 is found. Caraschi and Leão [53] found values of hardness around 62, while Koffi *et al* [54] obtained a hardness of 50.6 Shore D for pure HDPE. With the addition of ceramic reinforcement, the hardness is high, as  $\text{Al}_2\text{O}_3$  and SiC have higher hardness than ceramic HDPE, which has a greater hardness than polymeric materials [23,55].

The use of compatibilizers to improve the matrix/reinforcement interface allows the mechanical properties to be improved. The use of compatibilizers in composites in HDPE matrix composites allows the reinforcement phase to have greater adhesion with the matrix, resulting in improved mechanical properties [56].

## 4. Conclusions

This study evaluated HDPE matrix composites reinforced with alumina and silicon carbide particles and had their mechanical and ballistic properties. The ballistic test showed an improvement in the ballistic performance of samples with greater additions of ceramic reinforcement, resulting in samples A80 and A70 with higher energy absorption and lower DOP. The SEM images showed the mechanisms of fracture after impact, where the increase in the reinforcement content caused an increase in brittle fractures due to the greater presence of alumina and silicon carbide. The tensile and impact tests indicated a considerable reduction in the deformation and mechanical strength of samples A40, A50, and A60, as expected due to the ceramic reinforcements. Shore D hardness tests showed a significant increase in composite hardness due to additions of alumina and silicon carbide.

## Acknowledgements

This study was financed in part by the Brazilian Agency CAPES (Coordenação de Aperfeiçoamento de Pessoal de Nível Superior), Protocol #001.

## References

- [1] T. L. Castro-Espicalsky, S. T. Costa, B. M. Santiago, A. R. Freire, E. Daruge Júnior, F. B. Prado, and A. C. Rossi, "Craniofacial injuries by firearms projectiles: an analysis of 868 deaths in the five regions of Brazil," *Journal of Forensic and Legal Medicine*, vol. 69, p. 101888, 2020.
- [2] N. Rancic, M. Erceg, N. Radojevic, and S. Savic, "Medicolegal characteristics of firearm homicides in belgrade, serbia: before, during, and after the war in the former Yugoslavia," *Journal of Forensic Sciences*, vol. 58, pp. 1549-1553, 2013.
- [3] A. Amori, H. Sanaei-Zadeh, H. T. Zavarei, F. R. Ardestani, and N. Savoji, "Firearm fatalities. A preliminary study report from Iran," *Journal of Clinical Forensic Medicine*, vol. 10, pp. 159-163, 2003.
- [4] P. K. Stefanopoulos, O. T. Soupiou, V. C. Pazarakiotis, and K. Pazarakiotis, "Wound ballistics of firearm-related injuries - Part 2: Mechanisms of skeletal injury and characteristics of maxillofacial ballistic trauma," *International Journal of Oral and Maxillofacial Surgery*, vol. 44, pp. 67-78, 2015.
- [5] M. Justus, D. Hemenway, and M. Miller, "The relationship between alcohol consumption and the desire to own a firearm: an empirical study on citizens of São Paulo City, Brazil," *Public Health*, vol. 179, pp. 186-194, 2020.

- [6] A. B. Dresch, J. Venturini, S. Arcaro, O. R. K. Montedo, and C. P. Bergmann, "Ballistic ceramics and analysis of their mechanical properties for armour applications: A review," *Ceramics International*, vol. 47, pp. 8743-8761, 2021.
- [7] D. B. Rahbek, J. W. Simons, B. B. Johnsen, T. Kobayashi, and D. A. Shockey, "Effect of composite covering on ballistic fracture damage development in ceramic plates," *International Journal of Impact Engineering*, vol. 99, pp. 58-68, 2017.
- [8] P. H. P. M. Silveira, T. T. Silva, M. P. Ribeiro, P. R. R. Jesus, P. C. R. S. Credmann, and A. V. Gomes, "A brief review of alumina, silicon carbide and boron carbide ceramic materials for ballistic applications," *Academia Letters*, Article 3742, 2021.
- [9] M. P. Ribeiro, L. M. Neuba, P. H. P. M. Silveira, F. S. Luz, A. B. S. Figueiredo, S. N. Monteiro, and M. O. Moreira, "Mechanical, thermal and ballistic performance of epoxy composites reinforced with Cannabis sativa hemp fabric," *Journal of Materials Research and Technology*, vol. 12, pp. 221-233, 2021.
- [10] T. T. Silva, P. H. P. M. Silveira, M. P. Ribeiro, M. F. Lemos, A. P. Silva, S. N. Monteiro, and L. F. C. Nascimento, "Thermal and chemical characterization of kenaf fiber (hibiscus cannabinus) reinforced epoxy matrix composites," *Polymers*, vol. 13, 2016.
- [11] L. M. Neuba, R. F. P. Junio, M. P. Ribeiro, A. T. Souza, E. S. Lima, F. C. Garcia Filho, A. B. S. Figueiredo, F. O. Braga, A. R. G. Azevedo, and S. N. Monteiro, "Promising mechanical, thermal, and ballistic properties of novel epoxy composites reinforced with cyperus malaccensis sedge fiber," *Polymers*, vol. 12, 2020.
- [12] S. Naik, R. D. Dandagwhal, and P. K. Loharkar, "A review on various aspects of Kevlar composites used in ballistic applications," *Materials Today: Proceedings*, vol. 21, pp. 1366-1374, 2020.
- [13] J. L. Santos, R. L. S. B. Marçal, P. R. R. Jesus, A. V. Gomes, E. P. Lima, D. N. Rocha, M. A. P. Santos, L. F. C. Nascimento, S. N. Monteiro, and L. H. L. Louro, "Mechanical properties and ballistic behavior of LiF-added Al<sub>2</sub>O<sub>3</sub>-4 wt%Nb<sub>2</sub>O<sub>5</sub> ceramics," *Journal of Materials Research and Technology*, vol. 7, pp. 592-597, 2018.
- [14] P. H. P. M. Silveira, P. R. R. Jesus, M. P. R. Ribeiro, S. N. Monteiro, J. C. Oliveira, and A. V. Gomes, "Sintering behavior of Al<sub>2</sub>O<sub>3</sub> ceramics doped with pre-sintered Nb<sub>2</sub>O<sub>5</sub> and LiF," *Materials Science Forum*, vol. 1012, pp. 190-195, 2020.
- [15] S. N. Monteiro, A. C. Pereira, C. L. Ferreira, E. P. Júnior, R. P. Weber, and F. S. Assis, "Performance of plain woven jute fabric-reinforced polyester matrix composite in multilayered ballistic system," *Polymers*, vol. 10, pp. 230-239, 2018.
- [16] T. Goode, G. Shoemaker, S. Schultz, K. Peters, and M. Pankow, "Soft body armor time-dependent back face deformation (BFD) with ballistics gel backing," *Composite Structures*, vol. 220, pp. 687-698, 2019.
- [17] M. Bajya, A. Majumdar, B. S. Butola, S. K. Verma, and D. Bhattacharjee, "Design strategy for optimising weight and ballistic performance of soft body armour reinforced with shear thickening fluid," *Composites Part B: Engineering*, vol. 183, pp. 107721-107730, 2020.
- [18] R. E. Smallman, and R. J. Bishop, *Modern Physical Metallurgy and Materials Engineering*. Butterworth-Heinemann., 4th ed, 1999.
- [19] S. Hayun, V. Paris, R. Mitrani, S. Kalabukhov, M. P. Dariel, E. Zaretsky, and N. Frage, "Microstructure and mechanical properties of silicon carbide processed by Spark Plasma Sintering (SPS)," *Ceramics International*, vol. 38, pp. 6335-6340, 2012.
- [20] L. Zheng, W. Wei, X. Dong, C. Zhang, Y. Zeng, and H. Huan, "Microscopic wear study of the sintered diamond trepanning drill during machining alumina armor ceramics," *Ceramics International*, vol. 45, pp. 3986-3994, 2019.
- [21] S. M. Naga, H. F. El-Maghraby, M. Elgamhoudy, and M. A. Saleh, "Characterization and origin of failure of SiC/ZTA composites," *International Journal of Refractory Metals and Hard Materials*, vol. 73, pp. 53-57, 2018.
- [22] J. Chai, Y. Zhu, Z. Wang, Shen T, Y. Liu, L. Niu, S. Li, C. Yao, M. Cui, and C. Liu, "Microstructure and mechanical properties of SPS sintered Al<sub>2</sub>O<sub>3</sub>-ZrO<sub>2</sub> (3Y) - SiC ceramic composites," *Materials Science and Engineering: A*, vol. 781, p. 139197, 2020.
- [23] A. B. S. Figueiredo, E. P. Lima-Júnior, A. V. Gomes, G. B. M. Melo, S. N. Monteiro, and R. S. de Biasi, "Response to Ballistic Impact of Alumina-UHMWPE Composites." *Materials Research*, vol. 21, pp. 1-5, 2018.
- [24] F. J. Galindo-Rosales, F. J. Rubio-Hernández, and A. Sevilla, "An apparent viscosity function for shear thickening fluids," *Journal of Non-Newtonian Fluid Mechanics*, vol. 166, pp. 321-325, 2011.
- [25] J. Ding, P. J. Tracey, W. Li, G. Peng, P. G. Whitten, and G. G. Wallace, "Review on shear thickening fluids and applications," *Textiles and Light Industrial Science and Technology*, vol. 2, pp. 161-173, 2013.
- [26] D. Deepak, N. Goyal, P. Rana, and V. Gupta, "Effect of varying reinforcement content on the mechanical properties of hemp-recycled HDPE composites," *Materials Today: Proceedings*, vol. 18, pp. 5286-5291, 2019.
- [27] C. Y. Chee, N. L. Song, L. C. Abdullah, T. S. Y. Choong, and T. R. Chantara, "Characterization of mechanical properties: low-density polyethylene nanocomposite using nanoalumina particle as filler," *Journal of Nanomaterials*, vol. 10, pp. 1155-1160, 2012.
- [28] Z. Liao, M. Hossain, and X. Yao, "Ecoflex polymer of different Shore hardnesses: Experimental investigations and constitutive modelling," *Mechanics of Materials*, vol. 144, p. 103366, 2020.
- [29] F. M. B. Coutinho, I. L. Mello, and L. C. Santa Maria, "Polyethylene: main types, properties and applications," *Polymers*, vol. 13, pp. 1-13, 2003.
- [30] C. Kaufmann, D. Cronin, M. Worswick, G. Pageau, and A. Beth, "Influence of material properties on the ballistic performance of ceramics for personal body armour," *Shock and Vibration*, vol. 10, pp. 51-58, 2003.
- [31] M. A. Khan, Y. Wang, G. Yasin, A. Malik, F. Nazeer, W. Q. Khan, H. Zhang, and T. Ahmed. "Microstructure characteristic of spray formed 7055 Al alloy subjected to ballistic impact by two different steel core projectiles impact," *Journal of Materials Research and Technology*, vol. 8, pp. 6177-6190, 2019.

- [32] M. J. Oliveira, A. V. Gomes, A. R. Pimenta, and A. B. S. Figueiredo, "Alumina and low density polyethylene composite for ballistics applications," *Journal of Materials Research and Technology*, vol. 14, pp. 1791-1799, 2021.
- [33] ASTM D638-14, *Standard Test Method for Tensile Properties of Plastics*, ASTM International, West Conshohocken, PA, 2014.
- [34] ASTM D256-10, *Standard Test Methods for Determining the Izod Pendulum Impact Resistance of Plastics*, ASTM International, West Conshohocken, PA, 2018.
- [35] B. Jayendra, D. Sumanth, G. Dinesh, and M. R. Venkateswara, "Mechanical characterization of stir cast Al-7075/B4C/graphite reinforced hybrid metal matrix composites," *Materials Today: Proceedings*, vol. 21, pp. 1104-1110, 2020.
- [36] C. Y. Chee, N. L. Song, L. C. Abdullah, T. Choong, and T. R. Chantara, "Characterization of mechanical properties: low-density polyethylene nanocomposite using nanoalumina particle as filler," *Journal of Nanomaterials*, vol. 10, p. 215978, 2012.
- [37] ASTM D2240-15, *Standard Test Method for Rubber Property—Durometer Hardness*, ASTM International, West Conshohocken, PA, 2015.
- [38] S. A. B. Lins, M. C. G. Rocha, and J. R. M. D'Almeida, "Mechanical and thermal properties of high-density polyethylene/alumina/glass fiber hybrid composites," *Journal of Thermoplastic Composite Materials*, vol. 32, pp. 1566-1581, 2018.
- [39] A. Goulas, J. R. McGhee, T. Whittaker, D. Ossai, E. Mistry, W. Whittow, B. Vaidhyanathan, I. A. Reaney, J. C. Vardaxoglou, and D. S. Engstrom, "Synthesis and dielectric characterization of a low loss BaSrTiO<sub>3</sub>/ABS ceramic/polymer composite for fused filament fabrication additive manufacturing," *Additive Manufacturing*, vol. 55, p. 102844, 2022.
- [40] W. Wang, X. Bai, L. Zhang, S. Jang, C. Shen, and R. He, "Additive manufacturing of CsF/SiC composites with high fiber content by direct ink writing and liquid silicon infiltration," *Ceramics International*, vol. 48, pp. 3895-3903, 2022.
- [41] A. R. M. Vijay, C. T. Ratnam, M. Khalid, S. Appadu, and T. C. S. M. Gupta, "Effect of radiation on the mechanical, morphological and thermal properties of HDPE/rPTFE blends," *Radiation Physics and Chemistry*, vol. 177, pp. 109190-109200, 2020.
- [42] N. Kaya, E. Atan, and M. Sütçü, "Investigation of thermal properties of waste Tungsten Carbide (WC) loaded HDPE Matrix," *Materials Today Communications*, vol. 25, pp. 101547-101554, 2020.
- [43] F. S. Ortega, V. C. Pandolfelli, J. A. Rodrigues, and D. P. F. Souza, "Aspects of rheology and stability of ceramic suspensions. part iii: electro-stabilization mechanism for alumina suspensions" *Cerâmica*, vol. 43, pp. 281-282, 1997.
- [44] M. J. Oliveira, A. V. Gomes, and A. R. Pimenta, "Compósito de alumina e polietileno de baixa densidade, uma alternativa de aplicação em proteção balística," *Revista Militar de Ciência e Tecnologia*, vol. 38, pp. 61-67, 2021.
- [45] K. R. Dinesh, and G. Hatti, "Study of the effect of TiO<sub>2</sub>, CaCO<sub>3</sub> and Al<sub>2</sub>O<sub>3</sub> on mechanical properties of LDPE polymer composites fabricated by injection moulding technique," *Material Science Research India*, vol. 15, pp. 159-164, 2018.
- [46] I. Krásný, L. Lapčík, B. Lapčíková, R. W. Greenwood, K. Šafářová, and N. A. Rowson, "The effect of low temperature air plasma treatment on physicochemical properties of kaolinite/polyethylene composites," *Composites Part B: Engineering*, vol. 59, pp. 293-299, 2014.
- [47] K. Grison, T. C. Turella, L. C. Scienza, and A. J. Zattera, "Evaluation of the mechanical and morphological properties of HDPE composites with powdered Pinus taeda and calcined alumina," *Polimeros*, vol. 25, pp. 408-413, 2015.
- [48] L. J. Silva, T. H. Panzera, V. R. Velloso, and A. L. Christoforo, "Hybrid polymeric composites reinforced with sisal fibers and silica microparticles," *Composites Part B: Engineering*, vol. 43, pp. 3436-3444, 2012.
- [49] O. Faruk, and L. M. Matuana, "Nanoclay reinforced HDPE as a matrix for wood-plastic composites," *Composites Science and Technology*, vol. 68, pp. 2073-2077, 2008.
- [50] C. F. Martins, M. A. Irfan, and V. Prakash, "Dynamic fracture of linear medium density polyethylene under impact loading conditions," *Materials Science and Engineering: A*, vol. 465, pp. 211-222, 2007.
- [51] S. Alavitabari, M. Mohamadi, A. Javadi, and H. Garmabi, "The effect of secondary nanofiller on mechanical properties and formulation optimization of HDPE/nanoclay/nano CaCO<sub>3</sub> hybrid nanocomposites using response surface methodology," *Journal of Vinyl and Additive Technology*, vol. 27, pp. 54-67, 2021.
- [52] F. Awaja, S. Zhang, M. Tripathi, A. Nikiforov, and N. Pugno, "Cracks, microcracks and fracture in polymer structures: formation, detection, autonomic repair," *Progress in Materials Science*, vol. 83, pp. 536-573, 2016.
- [53] J. C. Caraschi, and A. L. Leão, "Evaluation of the mechanical properties of recycled plastics from solid urban waste," *Acta Scientiarum Maringá*, vol. 24, pp. 1599-1602, 2002.
- [54] A. Koffi, D. Koffi, and L. Toubal, "Mechanical properties and drop-weight impact performance of injection-molded HDPE/birch fiber composites," *Polymer Testing*, vol. 93, p. 106956, 2020.
- [55] A. B. S. Figueiredo, H. C. Vital, R. P. Weber, E. P. Lima-Júnior, J. G. P. Rodrigues, L. S. Aguilera, and R. S. de Biasi, "Ballistic tests of alumina-UHMWPE composites submitted to gamma radiation," *Materials Research*, vol. 22, pp. 1-7, 2019.
- [56] M. E. Mahmoud, M. A. Khalifa, R. M. El-Sharkawy, and M. R. Youssef, "Effects of Al<sub>2</sub>O<sub>3</sub> and BaO nano-additives on mechanical characteristics of high-density polyethylene," *Materials Chemistry and Physics*, vol. 262, p. 124251, 2021.
- [57] N. P. S. Chagas, V. O. Aguiar, F. C. G. Filho, A. B. H. S. Figueiredo, S. N. Monteiro, N. R. C. Huaman, and M. F. V. Marques, "Ballistic performance of boron carbide nanoparticles reinforced ultra-high molecular weight polyethylene (UHMWPE)," *Journal of Materials Research and Technology*, vol. 17, pp. 1799-1811, 2022.
- [58] M. Fejdyś, A. K. Jastrzębek, and K. Kośła, "Effect of Accelerated Ageing on the Ballistic Resistance of Hybrid Composite Armour with Advanced Ceramics and UHMWPE Fibres," *FIBRES & TEXTILES in Eastern Europe*, vol. 28, pp. 71-80, 2020.